

Design, Development of Magneto-Rheological Damper for Commercial Vehicles

Nitin P. Sherje¹, S. V. Deshmukh²

Department of Mechanical Engineering, Smt. Kashibai Navale College of Engineering¹

Department of Mechanical Engineering, Bapurao Deshmukh College of Engineering, Wardha²

n_sherje@rediffmail.com¹, svd4@rediffmail.com²

Abstract

The control of vibrations is a prime concern in an automobile because it may not only affects the comfort but also disturbs the stability of vehicle on road. The active suspension systems which has the better performance over the passive suspension system in terms of comfort as well as road handling has been introduced by an automobile industries in vehicles in the recent years. But, the drawbacks of this design are; high cost, high power requirement, more complication/mass of the apparatus needed for its operation and the need of frequent maintenance and repairs on some implementations etc. Hence, the vibration mitigation with semi-active control device has recently received considerable attention, because of its most appealing features; strong potential to control devices without imposing heavy power demands. The smart fluids, mainly Electro-rheological (ER) and Magneto-rheological (MR), which changes their properties in presence of an electric or magnetic field, are used in these devices. Hence, the work is focused on design, development and testing of MR damper. It also introduces the technique for optimizing the dimensions of damper based on the magnetic saturation of material.

Key Words: MR Damper, MR fluid, Magnetic Saturation

1. INTRODUCTION

The applications like machines, civil structures and vehicle undergo multiple sources of vibrations. The control of these vibrations is still to be a flourishing field for the researchers as it may hamper the integrity of structure, lead to misalignment and noise in case of machines and loses comfort in case of vehicles.

Generally, three types of controls are used in an automobile suspension system, passive, active and semi-active. Passive control is one which provides the constant damping, whereas active and semi-active control can provide variable damping effect. Recently, active suspension system consists of a force actuator which requires high external power to achieve the variable damping effect. Semi-active control requires a very less amount of power as compared to active control and provides the same effect. Hence, the semi-active control has received a significant attention of the researchers.

The semi-active control devices have been studied by the various researchers. Different types of devices used in semi-active suspension are MR damper and ER damper. Both MR and ER damper contain fluids whose rheology can change in presence of magnetic and electric field respectively.

Principle of magnetic design and a method for avoiding the magnetic saturation in design has been explained with the help of an example by Zhang *et al.*, 2006. Magnetic saturation was

analyzed by using Ansys Software. The results of theoretical and numerical methods were compared and found that, for a typical magnetic structure, the method of magnetic design is correct. The similar method can be adopted to analyze other magnetic loop to avoid the exploitation of magnetic performance of material and to magnify the force of damper by increasing eventually the magnetic potential of MR fluid in gap.

Ashfak *et al.*, 2009 has carried out the design, development and performance evaluation of MR damper. The rheology and theory behind MR fluids and application in vibration control have been discussed. It has been observed that, as

the voltage increases damping force increases for the constant interval of time. Damping force was very low for zero current and it increases gradually with increase in current. Similarly, controllable current was non zero for zero current also, it means yield stress never become zero. A single piston rod damper with an accumulator in order to satisfy the demand of automobile front suspension system has been developed. The damper structural parameters by integrated optimal design were obtained with the proper combination of magnetic circuit and structure. The formula has been derived to calculate the damping force of MR damper with an accumulator. *Fengchen et al., 2012* has been analyzed the magnetic coil by using finite element method. Further, investigated the properties of designed MR damper experimentally and provided a method for design and experimental study of automobile suspension system using MR damper. The initial bias force, adjustable ratio and maximum resistance of damper are directly affected by the gas pressure in energy storage cavity. It has been observed that, the damper performance with little error can be described in a better way by applying the least square method to fit the relationship between damping force current. MR damper with internal pressure control have been designed and developed. Three main design topics are covered, design of magnetic circuit, design of hydraulic system and development of an innovative pressure control apparatus. Analytical design approach was adopted and provided the equations for system design considering the desired force and stroke and maximum external dimensions. After analytical design of the circuit, finite element analysis method (FEM) has been performed to compare their results. The simulation has been carried out using FEM to check the saturation of different sections of structure.

Nicola et al., 2015 presented a prototype of MR damper. Several tests have been conducted to test the behaviour of this device. The result of the study might bring the new considerations that could lead an optimization of the properties of the damper and to its commercialization.

Weng et al., 2008 has been designed the damper using analytical flow solution. Annular gap through which the magnetized MR fluid is forced to flow from lower chamber to upper chamber in dampers is the most widely used configuration of MR damper. The damping force is produces when the fluid passes through gap. Hence, this arrangement in damper is approximated like a fluid flowing between two infinitely wide parallel plates. The authors have derived a general solution and the corresponding methodology to represent easily the fluid flow through annular gap with yield stress.

The presented work is focused on design and development of damper for commercial vehicles and uses the simple technique to optimize the dimensions of it. An experimental set up is designed and developed to investigate the performance of damper.

2.MAGNETO-RHEOLOGICAL DAMPERS

Semi-active control devices have an ability to change the amount of energy dissipated using small amount of power. These dampers are designed like the hydraulic dampers, wherein the controllable force is proportional to velocity. The possible range of damping characteristics obtained from regular passive damper can be extended with the help of semi-active dampers. The variable damping characteristics are achieved in it by creating a variable resistance in the form of position control valve such as solenoid valve, electro-rheological (ER) fluids and magneto-rheological fluids. Recently, some of these technologies are under research. The semi-active dampers use MR fluids or solenoid valves because of their advantages and cost effectiveness.

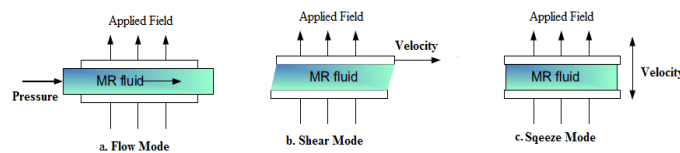


Fig 1: Different modes of operation [Gans, B.J. et al.,1996]

Magneto-rheological dampers have been disclosed in various US patents. These are mainly consists of an electromagnetic coil in close proximity with MR fluid flow as shown in fig 2. The arrangement is so made to create a

damping force that is adjustable by the current applied to the coil. The MR damper working principle is categories as: flow mode, shear mode and squeeze mode as shown in fig 1.

One of the most important applications of magneto-rheological fluid is magneto-rheological damper. The MR fluid has an ability to change apparent viscosity which idealizes it to use in dampers for controlling the vibrations. To change damping based on certain physical measurements like, velocity or acceleration, in order to better counteract and control the system dynamics, the real time adjustable systems can be developed. It has been observed that, the MR damper applications typically use the pressure driven flow (valve) mode of the fluid, or a combination of valve mode and direct-shear mode. Direct-shear mode is applicable for the dampers which do not require much force whereas, for high force requirement, mostly dampers with pressure driven modes can be used.

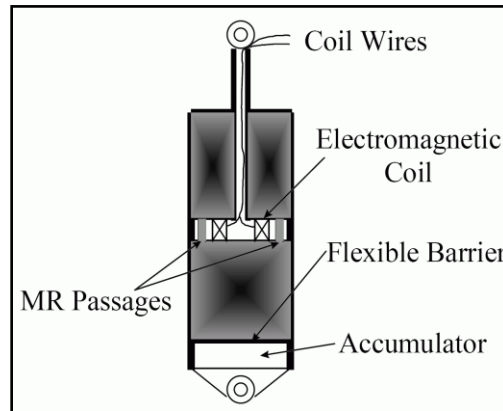


Fig 2: MR damper

The work presented is focused on design, development and testing of MR damper for commercial vehicle. The developed MR fluid is used for testing the damper. The dimensions of MR damper has been optimized by using a simple analytical approach. The saturation magnetization of different parts of designed MR damper is considered to optimize the dimensions.

4 DESIGN OF MR DAMPER

4.1 MR DAMPER GEOMETRY

The fig 3 and 4 shows the cylinder and piston of MR damper respectively.

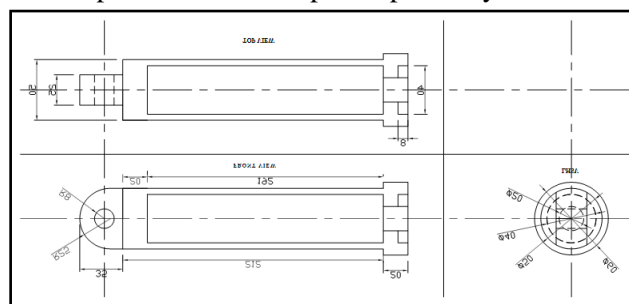


Fig. 3: Drawing of cylinder body

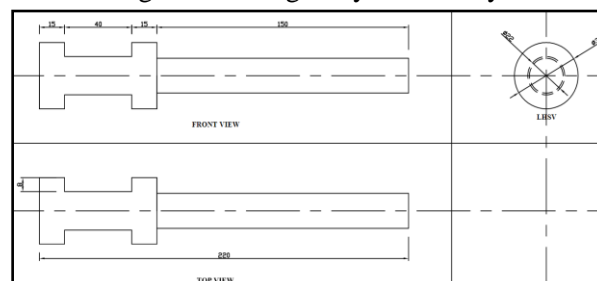


Fig. 4: Drawing of Piston body

Let,

Yield stress of MR fluid (τ_B) = 20 kPa

Viscosity of MR fluid in 'On State' (η) = 3 Pa-S

The different forces developed by the MR damper are shown in the fig 5. The forces can be divided into three stages of operation considering the parallel plate Bingham model. The first force is the controlling force correlate directly with the magnetic field through the yield stress. The controlling force of MR damper can be determined using the following equation [Nicola et al., 2015].

$$F_\tau = c \frac{\tau_B L_p A_A}{g} \text{sign}(V_d) \quad (4.1)$$

Where,

τ_B = Yield stress of MR fluid

L_p = Length of groove or axial activation length of piston

A_A = Effective cross section area of piston.

c = Coefficient which depends upon volumetric flow rate, viscosity and yield stress.

g = Fluid gap

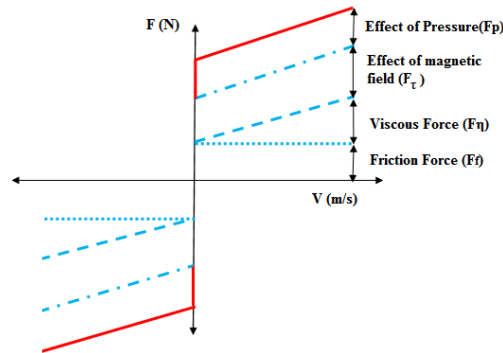


Fig: 5: The total damping force of MR damper is sum of: friction force, viscous force, controlling force and pressure driven force.

Effective cross section area of piston,

$$A_A = \frac{\pi}{4} \left[(\text{Piston Diameter})^2 - (\text{Piston Rod Diameter})^2 \right] \quad (4.2)$$

The second force is the viscous force, F_η depends upon the total length of piston, viscosity of MR fluid and rate of flow of fluid.

$$F_\eta = k \frac{12\eta Q L A_A}{w g^3} \quad (4.3)$$

Where,

Q = Rate of flow of fluid

η = Viscosity of fluid

w = Mean circumference of annular flow path

k = Constant depend upon volumetric flow rate and velocity.

$$k = 1 + \frac{w g V_d}{2Q} \quad (4.4)$$

Rate of flow of fluid (Q) of fluid,

$$Q = A_A \times V_d \quad (4.5)$$

Mean circumference of annular flow path,

$$w = \pi \left(\frac{\text{Inner Cylinder Diameter}}{2} + \frac{\text{Piston Diameter}}{2} \right) \quad (4.6)$$

Assumed the viscosity of fluid as $(\eta) = 0.3 \text{ Pa-S}$

Thus, viscous force can be calculated using the following equation,

$$\text{Viscous force}(f_\eta) = (1.060) \frac{12 \times \eta \times Q \times L \times A_A}{wg^3} \quad (4.7)$$

The force of friction (F_f) can be assumed for the safe design of damper as 250N [Nicola, 2015].

Total damper force is the sum of viscous force (F_η), friction force (F_f) and shear force (F_τ)

$$F_d = F_\eta + F_f + F_\tau$$

Hence, shear Force is,

$$F_\tau = F_d + F_\eta + F_f$$

By thumb rule dynamic range should be greater than 3

Thus, dynamic range is calculated using the following equation,

$$\text{Dynamic Range} = \frac{F_d}{F_\eta + F_f} = 4.22 \quad (4.10)$$

After finding the controlling force, the yield stress of the fluid was set as, $\tau_B = 20 \text{ Kpa}$ considering the nominal current as 1 amp [Nicola et. al., 2015].

Hence, the length of groove can be calculated by using following equation,

$$\text{Length of Groove } (L_p) = \frac{F_\tau g}{c \tau_B A_A} \quad (4.11)$$

Where, c is the coefficient which is depend upon the flow velocity profile and has the value range from 2 (for $\Delta P_\tau / \Delta P_\eta$ greater than 100) to 3 (for $\Delta P_\tau / \Delta P_\eta$ less than 1) [Carlson et. al, 1995]. Where, ΔP_τ and ΔP_η are field dependent and viscous pressure drop for single annular MR valve. In this work, the damper is designed considering pressure drop less than 1. Hence, the value of c is selected as 3.

4.2 MAGNETIC FIELD PARAMETERS

Magnetic field parameters mainly used are magnetic flux (ϕ), magnetic flux density (B), magnetic field intensity (H), magnetic potential (F) and magnetic reluctance. Magnetic flux is a measurement of total magnetic field passing through a given area whereas the magnetic flux density is an amount magnetic flux in an area taken perpendicular to the Magnetic flux's direction [Wang et. al, 2011].

Hence according to Ohm's law, the reluctance can be mathematically written as,

$$R = \frac{F}{\phi} = \frac{l}{\mu A} \quad (AT/Wb) \quad (4.12)$$

Magnetic field intensity,

$$H = \frac{NI}{l} \quad (AT/m)$$

Magnetic flux,

$$\begin{aligned} \phi &= \int_A B dA \\ &= BA \quad (Wb) \end{aligned}$$

Where, μ = Permeability of material = $\mu_0 \mu_r$

l = Average length of magnetic circuit

N = Number of turns of coil

A = Magnetic flow area

To optimize the dimensions of damper, the magnetic induction of MR fluid is obtained from the test curves. The saturation induction is assumed to be BA_{MR} . Assume that, the induction is uniform in the fluid gap and as the gap is much smaller than diameter of piston, the magnetic flux can be written as [Zhang H., 2006].

$$\phi = \int_A B dA = BA_{MR} \cdot \pi Da \quad (4.15)$$

Let, saturation magnetic induction for MR fluid, piston and cylinder are BA_{MR} , BA_{piston} , and $BA_{cylinder}$ respectively. Similarly, magnetic saturation areas are assumed as A_{MR} for MR fluid and A_1 , A_2 , A_3 for part 1, part 2 and part 3 of piston as shown in fig 6. To find out the saturation in the above mentioned parts, the saturation magnetic induction for MR fluid was 0.6 T and that of piston and cylinder was 2.5 T in general. The following relations can be written,

$$A_{MR} \cdot BA_{MR} = \pi Da \cdot BA_{MR} = 1103 \quad (4.16)$$

$$A_1 \cdot BA_{piston} = \frac{\pi}{4} [(D - 2h)^2 - d^2] BA_{piston} = 597 \cdot$$

$$A_2 \cdot BA_{piston} = \pi Da \cdot BA_{piston} = 4595 \quad (4.18)$$

$$A_3 \cdot BA_{cylinder} = \pi (D + g + \frac{t}{2}) t \cdot BA_{cylinder} = 1669$$

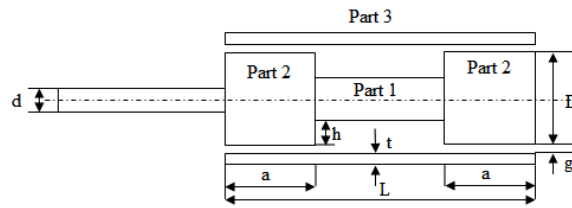


Fig 6: Piston with groove

Thus, from the above results it is clear that, the part 1 is being saturated first which in turn stops increase in the loop magnetic flux. The second saturated zone is MR fluid gap and which would directly affects the performance of damper. To avoid the saturation of part 1 of the piston first, the structural dimensions of the piston and cylinder needed modification. Hence, the magnetic flux of MR fluid gap has been a criterion for the structural modification. The saturation of MR fluid gap, cylinder and piston obtained simultaneously.

There is an insignificant effect on the magnetic flux because of the change in the parameters like 'a' and 'h', whereas the diameter of the rod cannot be modified because it is designed by the mechanical strength of rod. Also the thickness of cylinder is proportional to magnetic flux in part 3 i.e. cylinder and hence reducing the thickness of cylinder will reduce the magnetic flux which helps in saturating the cylinder first and it is desirable.

Modified structural dimensions $D = 45$ mm, $t = 3$ mm.

While modifying the thickness, the care is taken that the design of cylinder is safe.

Thus, the modified calculations are as under,

$$A_{MR} \cdot BA_{MR} = \pi Da \cdot BA_{MR} = 1272.34 \quad (4.20)$$

$$A_1 \cdot BA_{piston} = \frac{\pi}{4} [(D - 2h)^2 - d^2] \cdot BA_{piston} = 1210 \quad (4.21)$$

$$A_2 \cdot BA_{piston} = \pi Da \cdot BA_{piston} = 5301.43 \quad (4.22)$$

$$A_3 \cdot BA_{cylinder} = \pi (D + g + \frac{t}{2}) t \cdot BA_{cylinder} = 1120 \quad (4.23)$$

From the above calculations, it is clear that, the cylinder will get saturate first and it is obvious. Similarly, the saturation magnetic induction of part 2 of piston will always greater and never saturates before MR fluid gap. For the optimum performance of damper, the structural parameters like diameter of piston 'D', thickness of cylinder 't' and length 'b' of damper can be altered based on the typical magnetic loop. However, there are some limitations of traditional design approach as the saturation magnetic induction and relative permeability of material are not constant

but vary with the magnetic parameters. But the optimized parameters are sufficient to fulfill the requirement of the proposed study.

4.3 DESIGN OF MAGNETIC CIRCUIT

The main aim of magnetic circuit design is to determine the necessary number of turns of the magnetic coil to develop the required magnetic field which in turn develop the required damping force [Wang et. al, 2011, Zhang et. al, 2006]. The magnetic circuit design is based on the phenomenon that the conductor permeability is much greater than the insulative material. For an optimal design of MR damper it is essential to reduce the energy lost in the nonworking area in terms of fluxes in steel conduit. The entire magnetic circuit should have low reluctance, hence soft iron or high permeability steel should be used [Wang et. al, 2011]. While designing, the utmost care is taken about the same flux at all the cross section around the circuit. The iron particles may saturate because of the high flux density, hence the care is taken to provide the sufficient cross section for the iron around the coil.

The first step of the magnetic circuit design is to select proper magnetic material. Good magnetic design is also determined by magnetic structure design. The magnetic field form a loop in the magnetic material, if the magnetic loop get saturated anywhere, it will stop the continual increase of the whole loop. At the same time, the magnetic structure must ensure the accomplishment of structure function.

4.3.1 MAGNETIC RELUCTANCE (R_m)

It is the property of a material which is in magnetic equivalence with the electric property of resistance. The lower the reluctance, it is easier for the magnetic flux to flow through the core material. The materials which are easily magnetized have a low reluctance and high permeability and non magnetic materials have low permeability and high reluctance [Zhang et. al, 2006].

Magnetic reluctance can be expressed as,

$$R_m = \frac{l}{\mu A} = \frac{l}{\mu_0 \mu_r A} \quad (4.24)$$

Permeability of low carbon steel = $2000 \mu_0 = 0.00251 \text{ H/m}$ Permeability of free space (μ_0) = $4\pi \times 10^{-7} \text{ H/m}$

Permeability of MR fluid (μ_r) = $6 \mu_0 = 75.39 \times 10^{-7} \text{ H/m}$

For magnetic coil design the structure shown in fig (4.4) is divided in three parts, part 1 and part 2 belongs to piston and part 3 belongs to cylinder. Let, R_{m1} , R_{m2} and R_{m3} are the magnetic reluctance of parts 1, 2 and 3 of structure, whereas A_1 , A_2 and A_3 are magnetic flow area or cross sectional area of core.

Reluctance in part 1 is

$$R_{m1} = \frac{l}{\mu_0 \mu_r A_1} = \frac{L - 2a}{\mu_0 \mu_r \frac{\pi}{4} [(D - 2h)^2 - d^2]} \quad (4.25)$$

Reluctance in part 2 is

$$R_{m2} = \frac{l}{\mu_0 \mu_r A_2} = \frac{(D - d) / 2}{\mu_0 \mu_r \pi D a} \quad (4.26)$$

Reluctance in part 3 is

$$R_{m3} = \frac{l}{\mu_0 \mu_r A_3} = \frac{L - a}{\mu_0 \mu_r \pi (D + g + \frac{t}{2}) t} \quad (4.27)$$

From equations (4.25), (4.26) and (4.27)

Total Reluctance,

$$R = R_{m1} + R_{m2} + R_{m3} \quad (4.28)$$

The magnetic flux should be constant in the typical magnetic loop. The force of MR damper must ensure the normal operation of the vehicles, so one can get a reasonable gap width 'g' according to the fluid dynamics. And, from the formulation of concentric cylindrical magnetic pole, one can formulate the Magnetic Permeance as,

Magnetic Permeance,

$$A_g = \frac{2\pi\mu l}{\ln\left(\frac{R}{r}\right)} = \frac{2\mu_0\mu_{MR}\pi a}{\ln\left(1 + \frac{2g}{D}\right)} \quad (4.29)$$

Total Magnetic Potential,

$$F = \Phi\left(R + \frac{1}{A_g}\right) = \Phi(Rm_1 + 2Rm_2 + Rm_3 + \frac{\ln\left(1 + \frac{2g}{D}\right)}{\mu_0\mu_{MR}\pi a}) \quad \Phi = \text{Magnetic Flux} = 3\text{weber (Wb)} \quad (\text{Assumed})$$

According to whole magnetic potential, one can determine the upper limit of excitation current & number of turns.

Assume, $I_{max} = 2 \text{ Amp}$

Number of Turns of Coil,

$$N = \frac{\text{Magnetic Potential}(F)}{I_{max}} \quad (4.31)$$

Hence, the diameter of copper wire used for winding has been selected based on the current as,

$$d = 0.32 \text{ mm}$$

4.4 DEVELOPMENT OF MR DAMPER

MR damper consists of cylinder, piston and piston rod, coil assembly and oil seal. The cylinder is an external part of damper inside which piston and piston rod are incorporated. The single tube cylinder as shown in fig 7 is used in this work. It is made up of low carbon steel which has a high magnetic saturation and relative permeability. Eye is provided at bottom to bolt it to the required location. The assembly drawing of the damper is shown in fig. 9.



Fig 7: Actual Cylinder of MR damper

Piston of MR damper is wrapped into a magnetic coil as shown in fig 8. The function of piston in conventional damper and MR damper is same i.e. to force the fluid through valves or annular space. As shown in fig 8, a groove is provided on piston surface for coil. The required dimensions of groove were designed. The piston rod has been intentionally made hollow to allow the wire through it. Enamelled copper wire is used for coil and it is sealed with insulating material to avoid leakage in current. The same material has been used for piston as well as cylinder. Oil seal with cap at the top of cylinder is provided to avoid the leakage of oil through the cylinder.



Fig 8: MR damper piston

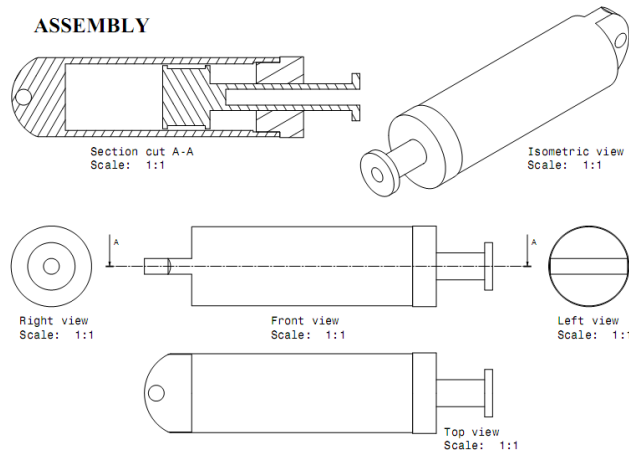


Fig 9: Assembly Drawing of MR damper

4.4 DEVELOPMENT OF EXPERIMENTAL SET UP

The experimental set-up has been developed to measure the damping force of semi-active MR damper at different current input. As discussed in the previous sections, variable damping can be achieved by using MR damper. Hence, an experimental set-up is developed wherein the arrangement is made to measure the change in damping force with respect to current and at same or different frequencies and amplitude. The provision is also made in the set up to change the current with change in the frequency of excitation or the displacement of damper automatically with the help of PID feedback controller. But, for the experimentation of present work, manual mode has been selected as the frequency of external excitation kept constant and observed the effect of change in current on the damping force.

Fig 10 shows the layout of the experimental set up developed for testing the performance of MR damper. The main components of it are vibration exciter, power oscillator, load cell, LVDT, current controller and data acquisition system (DAQ).

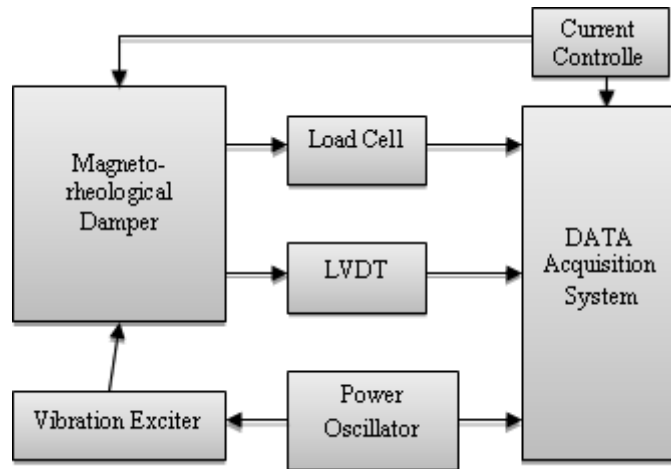


Fig 10: Layout of Experimental Set-up



Fig 11: Actual arrangement of Experimental Set-up

The following procedure has been adopted for testing the MR damper,

1. The actual arrangement of experiment set up is shown in fig 11. The one end of damper is connected to the vibration exciter and another end to load cell. LVDT is used to measure the displacement of cylinder. The Load cell and LVDT were connected to the control unit. The vibration exciter is connected to the power oscillator through which the frequency and amplitude of it can be varied. The power oscillator is further connected to control unit. The control unit consists of data acquisition system (DAQ) and current controller. The current controller is used to regulate the current passing through the electromagnetic coil. Data Acquisition System is provided to acquire the experimental data viz. damping force, displacement, current and frequency.
2. Initially, the frequency of vibration exciter has been set to a fixed value i.e. 10 Hz. No current has been supplied through the coil. In this case the damper was behaving like a passive damper.
3. In the next step, the current increased in the step size of 0.5 Amp and recorded the readings at every step.
4. The test has been conducted for three different developed MR fluid samples: MR1, MR3 and MR4
5. Thus, the plots have been drawn between damping force and time, damping force and displacement, damping force and velocity.
6. The dynamic range and the saturation limit of the proposed damper shall be determined with help of developed set up.

5. RESULTS

Test has been conducted to determine the parameters like damping force, displacement, velocity and acceleration at different current. The testing has been carried out at constant frequency (10 Hz) and by varying the current in the step size of 0.5 Amp. For all samples, damper started saturating from 1.5 Amp current and saturated at 2 Amp.

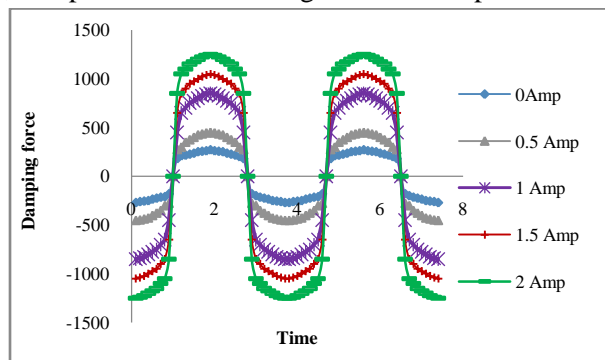


Fig 12: Damping force Vs Time for MR1 sample at different current input

The fig 12 shows the Damping force Vs Time plot for the current input in the step size of 0.5 Amp. It has been observed that, at 0 Amp current, the damper was behaving like a passive damper and as soon as the current increased the damping force also started increasing. There was a significant rise in the damping force from 0 Amp to 1.5 Amp. From 1.5 Amp it started increasing slowly and saturated at 2 Amp current. The damping force is 184 N at 0 Amp current and it has been increased to 1252 N at 2 Amp current.

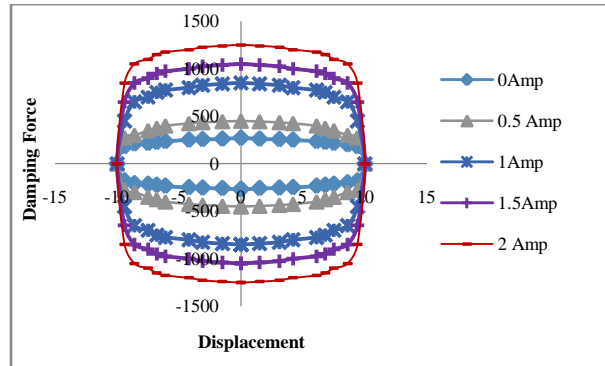


Fig 13: Damping Force Vs Displacement Plot at different current input for MR1

Fig 13 shows plot for damping force Vs displacement. The maximum displacement of the damper is 10 cm and

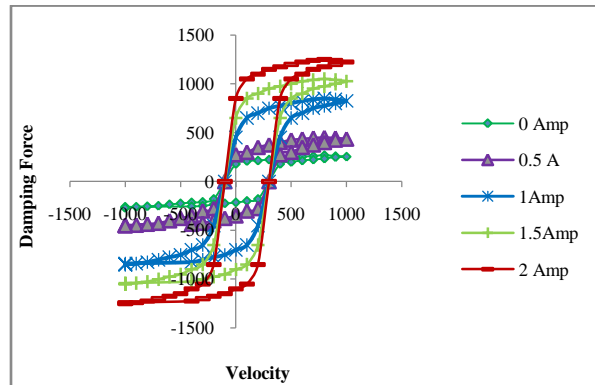


Fig 14: Damping Force Vs Velocity Plot at different current input for MR1

The fig 14 shows the Damping force Vs Velocity plot for the current input in the step size of 0.5 Amp. For the maximum velocity of 1005 mm/s, the damping force has been increased from 184 N to 1252 N.

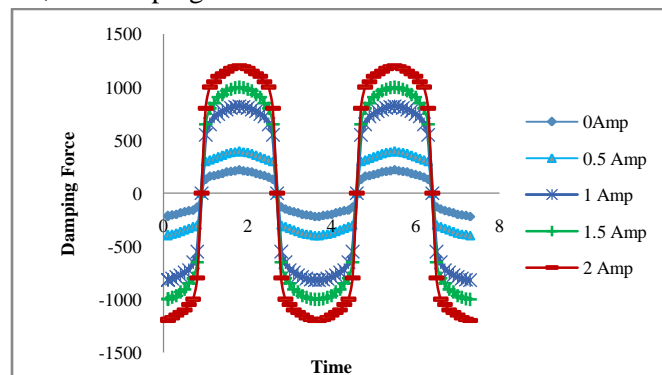


Fig 15: Damping Force Vs Time Plot at different current input for MR3

Fig 15 shows plot for force Vs time for MR 3 sample. The damping force is increased from 130 N to 1207 N.

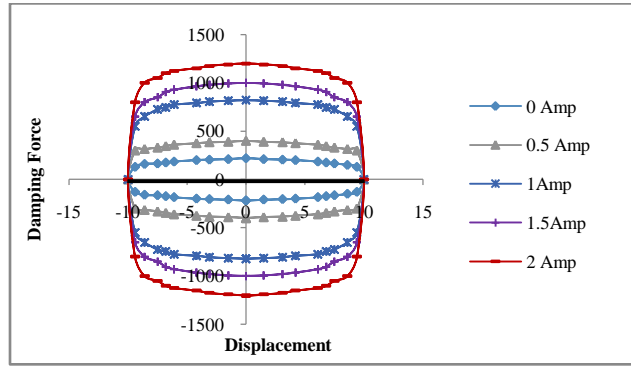


Figure 16: Damping Force Vs Displacement Plot at different current input for MR3

Fig 16 shows damping Force Vs displacement plot for MR 3 sample. For the maximum displacement of 10 mm, the damping force was increased from 130 N to 1207 N.

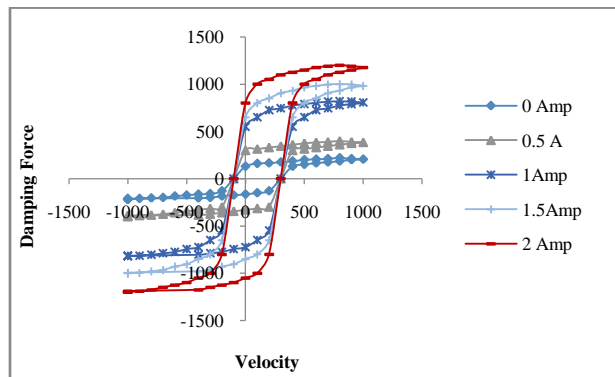


Figure 17: Damping Force Vs Velocity Plot at different current input for MR3

Fig 17 shows damping force Vs velocity for MR3 sample. The maximum velocity of 1005 mm/s, the damping force has been increased from 130 N to 1207 N.

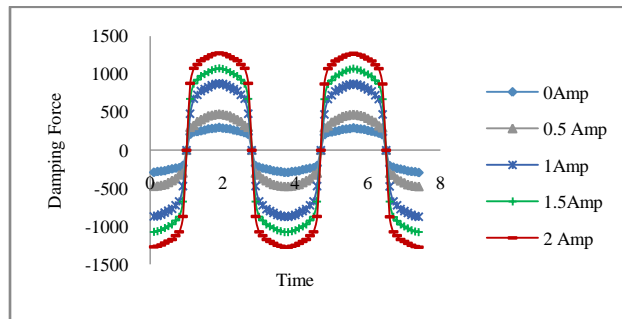


Figure 18: Damping Force Vs Time Plot at different current input for MR4

Fig 18 shows plot for force Vs time for MR3 sample. The damping force is increased from 201 N to 1276 N.

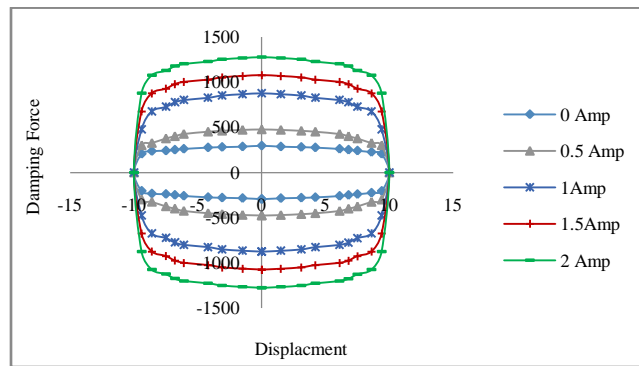


Fig 19: Damping Force Vs Displacement Plot at different current input for MR4

Fig 19 shows damping Force Vs displacement plot for MR 4 sample. For the maximum displacement of 10 mm, the damping force was increased from 201 N to 1276 N.

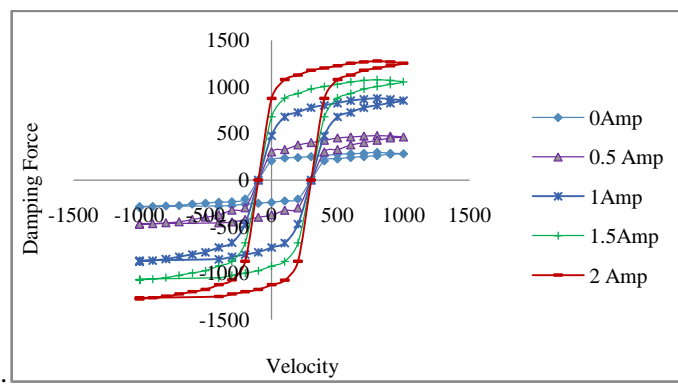


Figure 20: Damping Force Vs Velocity Plot at different current input for MR4

Fig 17 shows damping force Vs velocity for MR3 sample. The maximum velocity of 1005 mm/s, the damping force has been increased from 201 N to 1276 N.

6. CONCLUSION

It has been observed that at zero amp current the MR damper behaves like a passive damper and as soon as the current increases the damping force start increasing. It increases significantly upto a certain level and saturates thereafter. The components of damper should be saturated in the proper sequence to avoid its adverse effect on magnetization. The selection of material for damper components is very important. The material should have high saturation magnetization. The dynamic range of damper is not only depending upon the size but also the material used for damper.

REFERENCES

- [1] Spencer Jr. B. F, Dyke S. J., Sain M. K., Carlson J. D. (1996). Phenomenological Model of a Magneto-rheological Damper, Proceedings of the 12th Conference on Analysis and Computation, ASCE, Chicago, Illinois.
- [2] Butz T., Von Stryk O. (2002). Modeling and Simulation of Electro- and Magneto-rheological Fluid Dampers, ZAMM - Journal of Applied Mathematics and Mechanics. 82(1): 3-20.
- [3] Zhang H., Liao C., Chein W., Huang S. (2006). A magnetic design method of MR fluid dampers and FEM analysis of magnetic saturation. Journal of Intelligent Material Systems and Structures. 17(8-9).
- [4] Nicola G, Spaggiari A. (2015). Design of a novel magneto-rheological damper, with internal pressure control, Frattura ed Integrità Strutturale, 32:13-23.
- [5] Weng W. Chooi Design, modelling and testing of magneto-rheological (MR) dampers using analytical flow solutions, Volume 86, Issues 3-5, February 2008, Pages 473-482

- [6] Ashfak A., Saheed A., Rasheed KKA, Jaleel JA. (2009). Design, Fabrication and Evaluation of MR Damper, World Academy of Science, Engineering and Technology. International Journal of Mechanical, Aerospace, Industrial, Mechatronic and Manufacturing Engineering. 3, 5.
- [7] Spencer, B.F. Jr., S.J. Dyke, M.K. Sain, and J.D. Carlson, "Phenomenological Model for Magneto-rheological Dampers," ASCE J. Eng. Mech., vol. 123, pp. 230-238, 1997.
- [8] Carlson J. D., Weiss K. D. (1995). Magneto-rheological Materials Based on Alloy Particles, US Patent 5382373.
- [9] Fengchen Tu, Quan Yang, Caichun He, Lida Wang Experimental Study and Design on Automobile Suspension Made of Magneto- Rheological Damper" Sciverse science direct Energy Procedia 16 (2011), 417-425.
- [10]Strecker Z., B. Ruzicka. The Application of MR Dampers in the Field of Semi-active Vehicle Suspension. Mechatronics, Springer (2011), pp 149-154.